Available online at www.sciencedirect.com
SCIENCE DIRECT
Journal of Photochemistry and Photobiology A: Chemistry 182 (2006) 151–157
Journal of Photochemistry and Photobiology A:Chemistry
www.elsevier.com/locate/jphotochem

Temperature dependence of pyrene fluorescence spectra in aqueous solutions of C_nE_m ($C_{14}E_7$, $C_{16}E_7$, and $C_{16}E_6$) nonionic surfactant micelles

Chikako Honda*, Yumi Katsumata, Risa Yasutome, Sanae Yamazaki, Shigeaki Ishii, Keisuke Matsuoka, Kazutoyo Endo

Showa Pharmaceutical University, Department of Pharmacy, Higashi-Tamagawagakuen 3-3165, Machida, Tokyo 194-8543, Japan

Received 12 October 2005; received in revised form 23 January 2006; accepted 3 February 2006
Available online 24 March 2006

Abstract

Apparent hydrodynamic radii (R_{happ}) of nonionic surfactant micelles in aqueous solutions of hepta- and hexa-ethyleneoxide monoalkylether ($C_{14}E_7$, $C_{16}E_7$, and $C_{16}E_6$) were measured at 20–40 °C. Fluorescence spectra of pyrene in aqueous solutions of the nonionic surfactants were measured as a function of surfactant concentration and temperature. The cloud point of $C_{16}E_6$ was about 35 °C at concentration range of 10^{-3} to 10^{-2} M. However, even at a higher temperature than the cloud point, the fluorescence intensity ratio of pyrene monomer, I_{m1}/I_{m3}, in $C_{16}E_6$ solution behaves similarly to other surfactants ($C_{16}E_7$ and $C_{14}E_7$), indicating that the pyrene molecules reside in a similar location of surfactants. The slope for the temperature dependence of the I_{m1}/I_{m3} ratio also changed with the surfactant concentration, and the micelle size differed among the surfactants ($C_{16}E_6$, $C_{16}E_7$, and $C_{14}E_7$). The activation enthalpy of pyrene diffusion was evaluated using Stevens–Ban plot, and the value of 20–30 kJ mol^{-1} was obtained for surfactant concentrations of 5×10^{-4} to 10^{-2} M. The results were compared with those reported for ionic and nonionic surfactant micelles.

Keywords: Nonionic surfactant ($C_{14}E_7$, $C_{16}E_7$, $C_{16}E_6$) micelles; Pyrene fluorescence; Temperature dependence; Pyrene solubilization

1. Introduction

The fluorescence probe method is an effective technique for estimating the property and the time averaged locations of the solubilizates [1–9]. Pyrene is a suitable and effective fluorescence probe of its photophysical properties for understanding the structures of micelles, reversed micelles and microemulsions. Extensive reviews have been published for photophysics of pyrene [8], and for effectiveness of various photochemically active probes [9]. The intensity, I_{m1}, (0–0 band) of the pyrene fluorescence spectrum increases with the polarization of the probe environment. Then the ratio of I_{m1} to I_{m3} (2–0 band) shows the location of pyrene probe molecules in the mice lies [10–12]. The polarization of medium decreases with the rising temperature [13–15]. It is expected that the temperature dependence of the pyrene fluorescence emission intensity decreases with the temperature, since the rising temperature lowers the polarity of solvent [15].

Intermolecular excimer formation is affected under the solubilized number of pyrene molecules in a micelle. The number of pyrene probe in a micelle increased with the micelle aggregation number or the size [16]. The aggregation number and size of nonionic surfactant micelles depend on the temperature and surfactant concentrations. Formation of the pyrene dimer, which emits fluorescence in the vicinity of 470 nm, depends on the microviscosity of the pyrene molecules and the occupancy numbers of the solubilized pyrene in the micelles [17–23]. The excimer formation and the emitting fluorescence provide a suitable probe for investigating the properties of the micelles. Aoudia et al. reported the translational diffusion of the probe molecules by means of the temperature dependence of excimer–monomer emission [24]. Zachariasse discussed the kinetics and thermodynamics of intermolecular excimer formation, the temperature dependence of the excimer lifetime, the radiative rate constants of the excimer

* Corresponding author. Tel.: +81 042 721 1566; fax: +81 042 721 1565.
E-mail address: chikako@ac.shoyaku.ac.jp (C. Honda).

1010-6030/$ – see front matter © 2006 Elsevier B.V. All rights reserved.
doi:10.1016/j.jphotochem.2006.02.003

and monomer, and also the effects of solvent density for determination of excimer formation enthalpy and activation energy [25]. Recently, it has been recognized that water of solvation to surfactants and/or DNA is important roles for controlling structure, molecular recognition and dynamics in biological system [26–28].

In our previous paper [16], we studied the alkyl chain length dependence on pyrene location in micelles and maximum intensity of excimer in aqueous solutions of nonionic surfactants ($C_{10}E_7$, $C_{12}E_7$, $C_{14}E_7$, and $C_{16}E_7$) by means of fluorescence spectroscopy and light scattering technique. Rusdi et al. reported the relation between cmc and alkyl chain length of such surfactants as C_nE_8 ($n = 14$, 16, and 18) nonionic micelles [29]. Also Zhang et al. reported the ethyleneoxide chain length dependence of cmc about $C_{16}E_m$ ($m = 10$, 15, 20, and 24) micelles [30]. To our knowledge, there are few studies on the temperature dependence of fluorescence intensity of pyrene solubilized in nonionic micelles.

In the present study, fluorescence spectra of pyrene in aqueous solutions of hepta- and hexa-ethyleneoxide monoalkylether ($C_{14}E_7$, $C_{16}E_7$, and $C_{16}E_6$) were measured as a function of surfactant concentration and temperature. In nonionic surfactants, critical micelle concentration (cmc) and the cloud point are affected by hydration of the hydrophilic portion of the molecules. The I_{m1}/I_{m3} ratio for pyrene fluorescence and the excimer to monomer radiative intensity ratio, I_e/I_{m1}, of the probe over the wide surfactant concentration range from 10^{-7} to 10^{-2} M were analyzed using Stevens–Ban plot.

2. Experimental

Nonionic surfactant samples of hexa- and hepta-ethyleneoxide monoalkylether ($C_{14}E_7$, Lot no. 8006; $C_{16}E_6$ and $C_{16}E_7$, Lot no. 8011) were purchased from Nikko Chemicals (Tokyo, Japan). These samples were used without further purification. The purity of these surfactants was confirmed by attached chromatograms. Pyrene was purchased from Wako Pure Chemical Industries (Ohsaka, Japan) and was purified once by recrystallization in ethanol. SDS was purchased from Tokyo Kasei Kogyou (Tokyo, Japan) and was purified twice by recrystallization from 95% ethanol.

The cloud points were measured by suspending glass tube in water bath whose temperature was raised with 1 °C min^{-1}. The cloud point was determined by visual observation of turbidity.

After reaching the cloud point, the temperature was lowered gradually. The same cloud point was observed for both raising and lowering processes of temperature for the three surfactants used. The concentrations of surfactants for fluorescence measurement were ranged from 10^{-7} to 10^{-2} M. The SDS concentrations for fluorescence measurement were from 10^{-3} to 10^{-1} M in a phosphate buffer solution with ionic strength 0.034 M. Aqueous surfactant solutions with pyrene (1×10^{-4} M) were kept in a supersonic bath for approximately 2 h and then stirred continually for 3 days in a thermo-bath at 30 °C. The steady-state fluorescence emission spectra of pyrene solubilized in aqueous nonionic surfactant solutions were measured by means of a Fluorescence Photometer (FP-777 Jasco) with a xenon lamp. The temperature was from 25 to 45 °C, and fluorescence spectra were measured at every 5 °C. Before the measurement, the surfactant solutions were kept for 30 min at each temperature. All steady-state fluorescence spectra were obtained with an excitation wavelength of 335 nm and were scanned in the range of 350–550 nm with emission band width of 1.5 nm. The intensity of the third (I_{m3}) vibronic band over the first (I_{m1}) (0–0 vibronic band), I_{m1}/I_{m3} ratio (Fig. 4) located at 375 and 386 nm in the emission spectrum of monomeric pyrene provides an estimate of the polarity in a pyrene environment. The fluorescence intensity (I_e) in the region of 450–550 nm, ascribed to excimer emissions, was measured at a wavelength of 470 nm.

The hydrodynamic radii of micelles were measured by means of a light scattering photometer. Dynamic light scattering was performed by using ALV-5000 apparatus manufactured by ALV with a Nd-YAG semiconductor laser operated at 532 nm as a light source. Surfactants solutions were optically purified through a teflon filter with the nominal pore size of 0.2 μm. Stock surfactant solutions were added in a dust free optical cell and these cells were flame sealed under mild vacuum. Before the light scattering measurement, samples were kept at a temperature from 20 to 45 °C every 5 °C for about 30 min. The autocorrelation functions were measured, and analyzed by the cumulant expansion. Diffusion coefficients were determined and the hydrodynamic

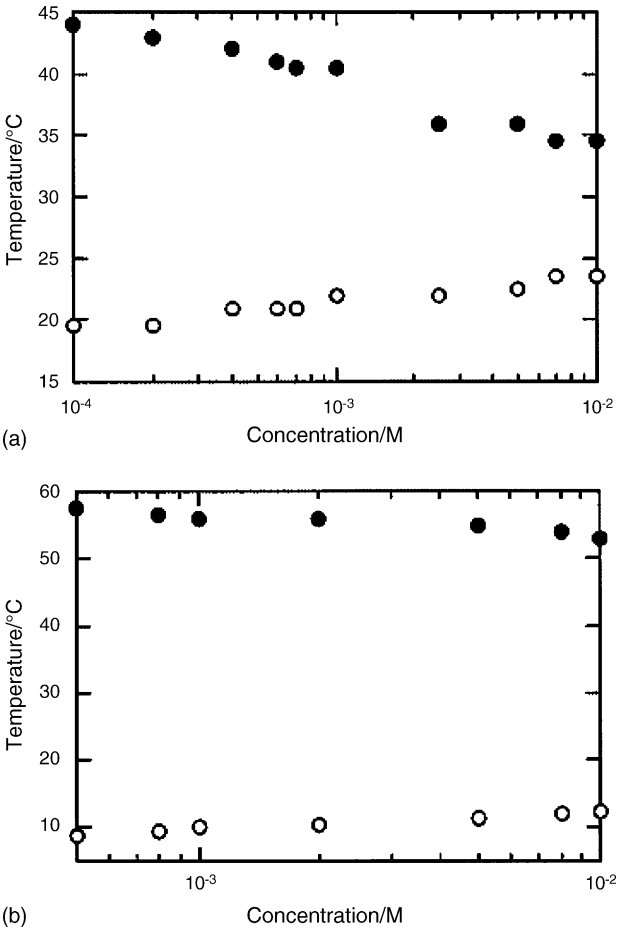

Fig. 1. Cloud point (●) and dissolution temperature (○) for $C_{16}E_6$ (a) and $C_{16}E_7$ (b).

radius was calculated with the Stokes–Einstein equation assuming sphere micelles.

3. Results and discussion

The cloud points of $C_{16}E_6$ and $C_{16}E_7$ are shown in Fig. 1(a) and (b). The cloud point of $C_{16}E_6$ was low at about 35 °C for the higher concentration range from 2×10^{-3} to 10^{-2} M, the temperature of dissolution being 22–24 °C. Therefore, the micelle forming temperature region was limited for $C_{16}E_6$ compared with $C_{16}E_7$ or $C_{14}E_7$ at the concentration range of 10^{-4} to 10^{-2} M. Toerne et al. suggested that the minor changes of polyoxyethynene (PEO) chain length caused significant changes for the values of cloud point and cmc in system of Triton X-35, 100, 114, and 405 [31]. The present results on the cloud points for $C_{16}E_6$ and $C_{16}E_7$ are consistent with those of their observations. The cmc of these surfactants are shown in Table 1 [32,33]. As the carbon number of alkyl chain increases, the cmc shifts lower concentration. However, the cmc is little affected by one ethyleneoxide unit.

Apparent hydrodynamic radii (R_{happ}) of $C_{16}E_7$ and $C_{14}E_7$ micelles increased with increasing surfactant concentration and with rising temperature (Fig. 2(a) and (b)). At lower temperatures (20 and 25 °C), $C_{14}E_7$ micelles sizes were remained almost unchanged. However, the aggregation number of these surfactants increased with rising temperature. The $C_{16}E_7$ micelles sizes were remained constant at 20 °C, but at other temperatures R_{happ} increased with the surfactant concentration and reached a constant value at about 0.005 M. The temperature dependence of R_{happ} is more remarkable for $C_{16}E_7$ micelles than for $C_{14}E_7$.

Fluorescence spectra of solubilized pyrene in the $C_{16}E_7$ micelles at 20 °C are shown in Fig. 3 at several concentrations. The pyrene monomer fluorescence intensities (I_{m1} and I_{m3}) increased with the surfactant concentration and pyrene excimer fluorescence intensity (I_e) reached a maximum value and then decreased with the concentration. The concentration dependence of the I_{m1}/I_{m3} ratio is shown in Fig. 4. The I_{m1}/I_{m3} ratio was approximately constant below the cmc, and decreased gradually around the cmc, and finally it reached an approximately constant value. As shown in Fig. 4, the I_{m1}/I_{m3} ratio of the pyrene fluorescence in phosphate buffer solution (0.034 M ionic strength) of SDS micelles exhibited sharp decrease at the cmc. SDS forms nearly the same size micelles at the cmc and above the cmc, the number of the micelles increases with the concentration. In contrast, at the lower temperature, the I_{m1}/I_{m3} ratio for $C_{16}E_7$ decreased more sharply with concentration. At higher temperature, relatively small micelles are formed at cmc, because the

Table 1
cmc of C_nE_m surfactants at 25 °C

Sample	cmc × 10^5 M	
	This work	Literature value[a]
$C_{14}E_7$	1.0	0.90
$C_{16}E_7$	0.30	0.20
$C_{16}E_6$	0.40	0.20

[a] Obtained from Refs. [32,33].

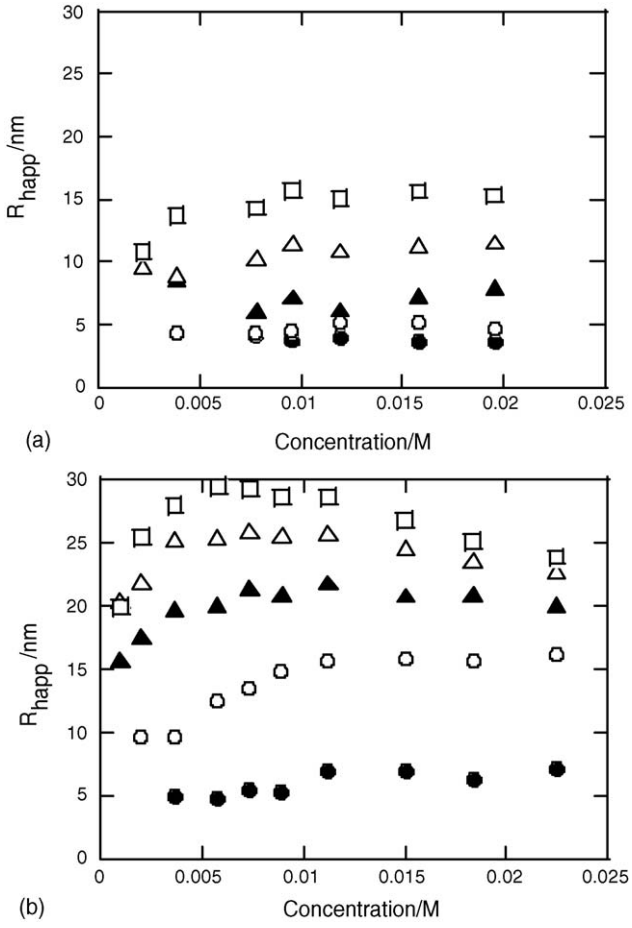

Fig. 2. Apparent hydrodynamic radii dependence on concentration and temperature for $C_{14}E_7$ (a) and $C_{16}E_7$ (b). 20 °C (●), 25 °C (○), 30 °C (▲), 35 °C (△), and 40 °C (□).

cmc is at a very low (see Table 1). Therefore, these micelles, which are formed at the cmc, grow its size with increasing concentration. $C_{16}E_6$ shows a similar behavior in I_{m1}/I_{m3} ratio above the cloud point. This fact reveals that pyrene molecules solubilized in a similar location above the cloud point. Turro and

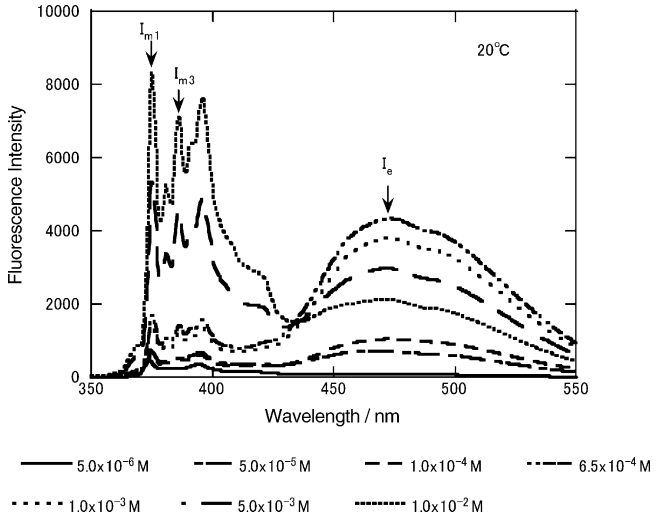

Fig. 3. Fluorescence spectra at various concentrations for $C_{16}E_7$ at 20 °C.

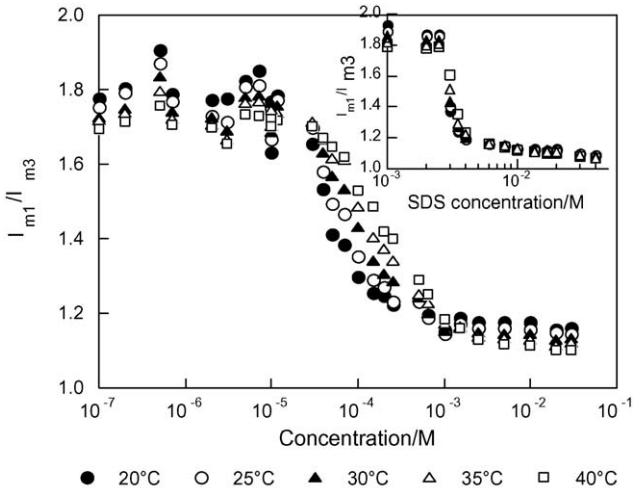

Fig. 4. Concentration dependence of I_{m1}/I_{m3} at various temperatures for $C_{16}E_7$. 20 °C (●), 25 °C (◯), 30 °C (▲), 35 °C (△), and 40 °C (□). Inset figure is I_{m1}/I_{m3} for SDS.

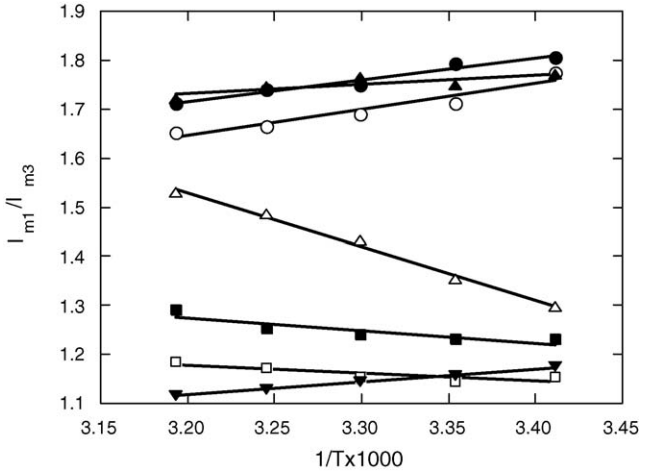

Fig. 5. Reciprocal temperature dependence of I_{m1}/I_{m3} at various concentrations for $C_{16}E_7$. 2×10^{-7} M (●), 3×10^{-6} M (◯), 1×10^{-5} M (▲), 1×10^{-4} M (△), 5×10^{-4} M (■), 1×10^{-3} M (□), and 1×10^{-2} M (▼).

Kuo showed the evidence for the existence of micelles above the cloud point by means of fluorescence measurement using pyrene-3-carboxialdehyde probe in the poly(ethylene glycol)$_n$-nonylphenyl ether micelles [34].

Below the cmc and at concentration above 10^{-3} M, higher values for the I_{m1}/I_{m3} ratio of pyrene fluorescence were observed at lower temperature. In the intermediate concentration region between cmc (near 10^{-5} M) and 10^{-3} M, higher values of the I_{m1}/I_{m3} ratio were observed at higher temperature. The trends are opposite to those found below cmc and at concentrations above 10^{-3} M. As pointed out by Nakajima [10,35,36], this phenomenon can not be explained only by the polarity of the solvent. He concluded from the pyrene fluorescence spectra in the *o*-, *m*- and *p*-dichlorobenzenes at 60 °C that these spectra could not consistently be explained only by the effects of solvent dipole and suggested that the spectral intensities would be affected also by the structure of solvent molecules.

Fluorescence monomer emission intensities, I_{m1} and I_{m3}, increased with temperature at the surfactant concentration range from 10^{-7} to 10^{-5} M, and decreased with rising temperature at higher concentration than about 10^{-4} M. The excimer fluorescence intensity was very low below the cmc, and remained unchanged with rising temperature. Above the cmc, the excimer fluorescence intensity decreased by temperature quenching and/or decreased solvent polarity. Although the solvent polarity lowers with rising temperature, [13–15] the emission intensity increases below the cmc. According to the report by Wauchope et al., the solubility of pyrene increases with temperature, and the average concentration is 0.127×10^{-6} M at 22.2 °C and 0.390×10^{-6} M at 44.7 °C, respectively [36,37]. Then the fluorescence intensity is directly influenced by the solubility and increases with the temperature at low surfactant concentration. On the other hand fluorescence intensity decreased with the temperature at the higher surfactant concentration than 10^{-4} M [13–15]. At these surfactant concentrations, most of the pyrene molecules solubilized in the micelles. Therefore, even if the pyrene solubility effects on the fluorescence intensity, the effect will be small.

Fig. 5 shows the I_{m1}/I_{m3} ratio against reciprocal absolute temperature for several concentrations of $C_{16}E_7$ surfactant. A good linear relationship between the ratio and $1/T$ was established for each concentration. The I_{m1}/I_{m3} ratio shows the positive slope at higher than 1×10^{-3} M and at lower concentrations than 3×10^{-5} M and shows a negative slope at intermediate concentration from 3×10^{-5} to 1×10^{-3} M. Fig. 6 shows the slopes of I_{m1}/I_{m3} ratio against concentration of $C_{16}E_6$, $C_{16}E_7$, and $C_{14}E_7$. The slopes exhibited approximately the same values up to 10^{-5} M, and then decrease rapidly at about from 10^{-5} to 10^{-4} M. It reached a minimum value and then increased gradually with the surfactant concentration. After 2×10^{-3} M, the slope became positive, and did not change at higher concentration. Waris et al. reported that increased thermal agitation and a weakening of the pyrene-solvent interactions were responsible

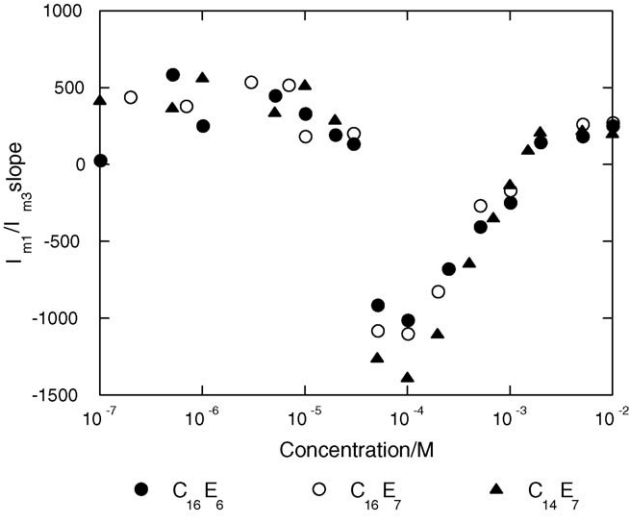

Fig. 6. The slope of I_{m1}/I_{m3} against temperature. $C_{16}E_6$ (●), $C_{16}E_7$ (◯), and $C_{14}E_7$ (▲).

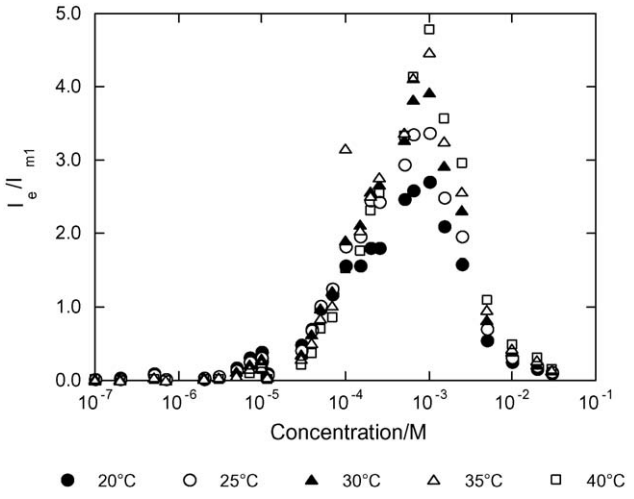

Fig. 7. Concentration dependence of I_e/I_{m1} at various temperatures for $C_{16}E_7$. 20 °C (●), 25 °C (◯), 30 °C (▲), 35 °C (△), and 40 °C (□).

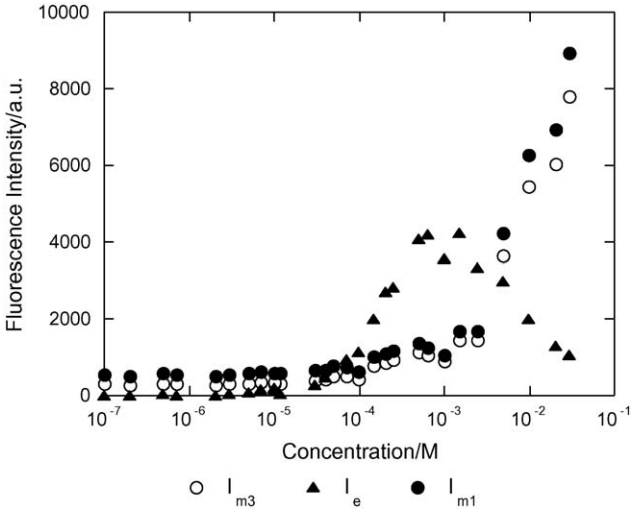

Fig. 8. Concentration dependence of pyrene monomer and excimer fluorescence intensity at 25 °C. I_{m1} (●), I_{m3} (◯), and I_e (▲).

for decrease in the intensity of 0–0 band, I_{m1}, relative to that of band I_{m3} at higher temperature, and noted that the I_{m1}/I_{m3} ratio of pyrene in a number of solvents exhibited changes with temperature [38]. Hara et al. have reported that the intensity ratio for pyrene depends on temperature, and that the increase of the ratio is related with increase of polarity [39]. They rationalized the effect in terms of thermal agitation. For the temperature dependence of the I_{m1}/I_{m3} ratio for $C_9P_hE_n$ at the 2×10^{-3} M in the aqueous solution with the negative slope, Turro and Kuo explained that the negative slope corresponded to the decrease in polarity experienced by pyrene in the homogeneous environment, because the solvent polarity decreased with the temperature [34]. Ndou et al. reported the effect of temperature on the I_{m1}/I_{m3} ratio in premicellar and micellar TX-405 solutions [40]. The slope of the I_{m1}/I_{m3} ratio against temperature exhibited negative for all of the measured concentrations. They explained that this fact was attributed to thermal agitation which reduced the intermolecular interactions of short range in the solvent. In the intermediate concentration, I_{m1}/I_{m3} ratio exhibits a remarkably negative slope (the same trends as stated also for Fig. 5) because the instability of pyrene in the micelles by thermal agitation is greater than the effect of the solvent polarity. However, after the micelle size reaches a constant value, the concentration dependence of I_{m1}/I_{m3} ratio shows a positive slope. When the micelle concentration is higher, pyrene molecules distribute preferentially in these micelles. The number of pyrene molecules in a micelle decreases, then the slope of the I_{m1}/I_{m3} against concentration turns into positive. Namely, pyrene molecules in the micelles have a Poisson distribution [41,42].

Fig. 7 shows the fluorescence intensity ratio, I_e/I_{m1}, of excimer to monomer of pyrene against $C_{16}E_7$ concentration. The ratio showed a maximum, and then decreased with the surfactant concentration. The excimer fluorescence intensity I_e depends on the number and the size of micelles in addition to the pyrene molecules in a micelle. It is generally known that the number of micelles increases for C_nE_m at high surfactant concentrations at lower temperature. Since total number of pyrene molecules is kept constant through this experiment, and micelle size increases with temperature (see Fig. 2), consequently the I_e increases with temperature, if the number of solubilized pyrene molecules in a micelle is enough. As the number of micelle increases, pyrene molecules distribute widely in the micelles under a constant pyrene concentration [41,42]. The maximum I_e/I_{m1} ratio was observed at about 10^{-3} M surfactant irrespective of temperatures. The reason responsible for the fact will be explained in the following. Almost all pyrene molecules of 10^{-4} M were solubilized in the micelles at 20 °C. Even if the micelle sizes increase with rising temperature, no pyrene molecules exist in the solution, since pyrene concentration is fixed. Then excimer fluorescence intensity shows the maximum at the same concentration of surfactants. If more pyrene molecules exist in the solution, maximum excimer fluorescence intensity shifts lower surfactants concentrations with temperature.

The fluorescence intensities of monomer and excimer are compared at 25 °C with the concentration in Fig. 8. The excimer fluorescence intensity increased at higher concentration than 10^{-5} M, reached maximum at about 5×10^{-4} M and decreased after the maximum value. On the other hand, monomer fluorescence intensities (I_{m1} and I_{m3}) increased gradually at lower concentration and increased rapidly at higher concentration than 10^{-3} M. This suggests that the monomer concentration does not increase at the same time as the excimer concentration increases. As the number of micelles increases with surfactant concentration, the number of pyrene in a micelle decreases, which reflects the I_e in Fig. 8.

Fig. 9 shows the Arrhenious type plot (Stevens–Ban plot) [43], a logarithm of I_e/I_{m1} of pyrene fluorescence in $C_{16}E_7$ micelles solution against reciprocal temperature. The $\ln(I_e/I_{m1})$ versus reciprocal absolute temperature reached a positive slope at the lower concentration and had a gentle slope with increasing concentration. At a higher concentration than 1×10^{-4} M, the slope turned into negative.

The dependence of I_e/I_{m1} on the reciprocal temperature based on the two state model was well presented by Birks et

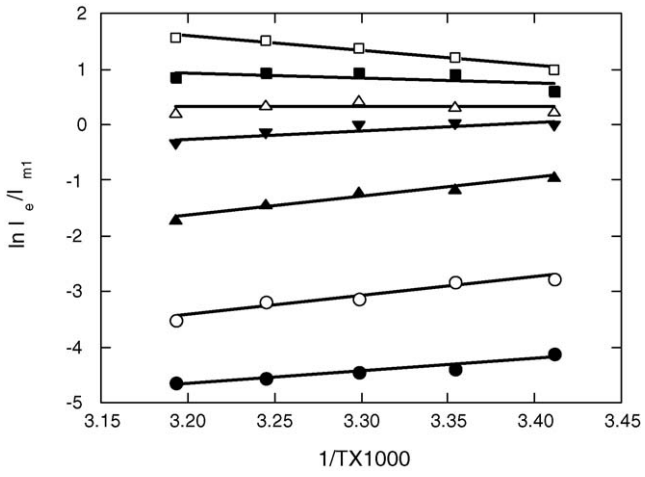

Fig. 9. Reciprocal temperature dependence of I_e/I_{m1} at various concentrations for $C_{16}E_7$. 2×10^{-7} M (●), 3×10^{-6} M (○), 1×10^{-5} M (▲), 5×10^{-5} M (▼), 1×10^{-4} M (△), 2×10^{-4} M (■), and 1×10^{-3} M (□).

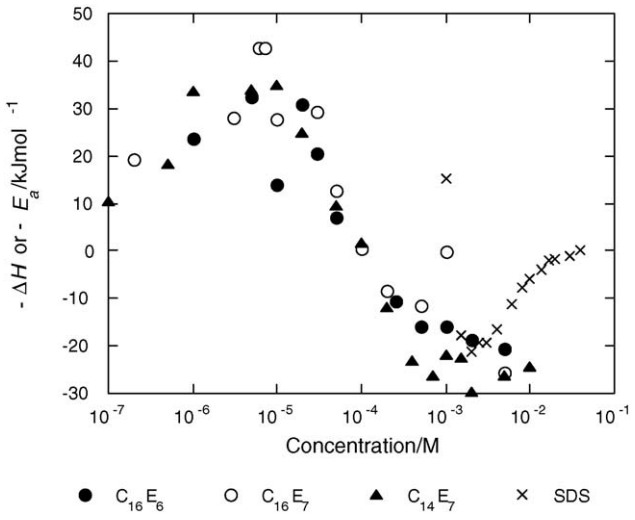

Fig. 10. Excimer formation enthalpy (ΔH) and excimer activation energy at various surfactant concentrations. $C_{16}E_6$ (●), $C_{16}E_7$ (○), $C_{14}E_7$(▲), and SDS (×).

al. [44–47]. Aoudia et al. applied this model to analyze the fluorescence from isomeric haxadecylbenzenesulfonates, and showed both positive and negative temperature dependence of I_e/I_{m1} against $1/T$ for a particular surfactant concentration [24]. Zachariasse examined the kinetics and thermodynamics of fluorescence ratio, I_e/I_{m1}, of aromatic hydrocarbons, based on the two state model and discussed the fluorescence ratio and excimer formation enthalpy ΔH and the activation energy E_a [25]. The excimer formation enthalpy ΔH is concerned with the activation energies E_a of excimer formation and excimer dissociation E_d as $(E_d - E_a)/R = -\Delta H/R$. Assuming the diffusion controlled excimer formation, the mechanism of the kinetics of the excimer formation may be represented by

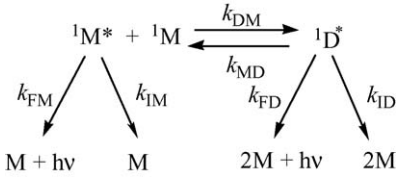

where M and D denote monomers and dimers, and asterisks denote an excited state. k_{FM}, k_{FD}, k_{DM}, and k_{MD} are the rate constants of monomer fluorescence, excimer fluorescence, excimer formation, and excimer dissociation, respectively. k_{IM} and k_{ID} are the rate parameters of nonradiative transition of monomer and excimer.

It is assumed that k_{DM}, k_{MD}, k_{FM}, and k_{FD} do not depend on the temperature, at low temperature, the excimer to monomer emission intensity ratio is given as

$$\frac{I_e}{I_{m1}} = \frac{k'_{DM}}{k_{FM}} \exp\left[\frac{-E_a}{RT}\right] \quad (1)$$

where k'_{DM} and E_a are the frequency factor and activation energy of excimer formation, respectively, and R is gas constant.

At high temperature region, the I_e/I_{m1} ratio is given as

$$\frac{I_e}{I_{m1}} = \frac{k_{FD}k'_{DM}[^1M^*]}{k_{FM}k'_{MD}} \exp\left[\frac{-\Delta H}{RT}\right] \quad (2)$$

where ΔH is the excimer formation enthalpy change associated with excimer formation and k'_{DM} is the frequency factor. In this experiment, the slope for Arrhenius type plot of I_e/I_{m1} against $1/T$ depended on the surfactant concentration, i.e., the positive slope was found for relatively lower surfactant concentrations, and the negative one for high concentrations. The activation energy to form an excimer is obtained from the negative slopes. Positive slopes obtained in the concentration range of 10^{-5} M (cmc) to 10^{-4} M indicates that the proportions of excimers decrease with rising temperature. Fig. 10 shows the $-\Delta H$ and $-E_a$ of pyrene in the $C_{16}E_6$, $C_{16}E_7$, $C_{14}E_7$ and SDS micelles with the concentration of surfactants. Although the sizes of nonionic micelles changed with concentration and temperature, the slope of I_e/I_{m1} against $1/T$ showed similar tendency to the concentration. It seems that $-\Delta H$ or $-E_a$ once passes maximum at about 10^{-5} M, then it decreases with the concentration. Excimer fluorescence intensity exhibited maximum at about 5×10^{-4} M (see Fig. 8). At these surfactant concentrations, excimer formation enthalpy of pyrene in the micelles shows large values. Aoudia et al. reported the activation energy of pyrene in the alkylbenzenesulfonate surfactant, the value was 37.6 kJ mol^{-1} [24]. Galla and Sackmann reported activation energy for pyrene was 36.8 kJ mol^{-1} by the diffusion coefficient in the diparmitoyllecithin membranes [48]. Martinho et al. reported the activation energy 36 ± 1 kJ mol^{-1} by the diffusion coefficient of pyrene in cyclohexanol [49]. Malliaris et al. reported the activation energies of pyrene in the various ionic, zwitterionic, and Triton X-100 surfactants from the fluorescence decay rate, which were from 24.2 to 33.1 kJ mol^{-1} except SDS and Triton X-100 [50]. The activation energy of pyrene has been reported to be 19.2 kJ mol^{-1} for a system of BSA–SDS complexes [51]. In this experiment at higher concentration than about 10^{-3} M, the E_a value of 20–30 kJ mol^{-1} was obtained, which was a little lower than the value of Aoudia et al. and in agreement with the value of Malliaris et al. Recently, the activation energy for diffusion of 4-aminophthalimide (4-AP) in aqueous solution of Triton X-

100 was reported to be $37.7 \pm 4.2\,kJ\,mol^{-1}$ based on lifetime measurement of fluorescence [52]. 4-AP probe has polar (or hydrophilic) functional groups in the molecule and is different from pyrene. In present study, the enthalpy of pyrene diffusion was evaluated in nonionic surfactant micelles. By comparing the enthalpy with the reported data, the remarkable difference has not been found between the pyrene diffusion in nonionic and ionic micelles.

4. Conclusion

The cloud points and dissolution temperature for $C_{16}E_6$ and $C_{16}E_7$ were estimated. The hydrodynamic radii of $C_{16}E_6$ and $C_{16}E_7$ micelles were found to be nearly constant against the surfactant concentration at low temperature region (20 and 25 °C), while they increased at high temperature (30, 35, and 40 °C). The pyrene fluorescence spectra were measured at 20, 25, 30, 35, and 40 °C in aqueous solution of various concentrations (10^{-7} to 10^{-2} M) of the nonionic surfactants ($C_{16}E_6$, $C_{16}E_7$, and $C_{14}E_7$). Surfactant concentration dependence of I_{m1}/I_{m3} ratio changed moderately compared with that of ionic surfactant SDS micelles. The slope for the I_e/I_{m1} ratios against reciprocal temperature were analyzed for various surfactant concentrations, and the activation enthalpy of pyrene diffusion was evaluated.

References

[1] P.P. Infelta, Chem. Phys. Lett. 61 (1979) 88–91.
[2] A. Yekta, M. Aikawa, N.J. Turro, Chem. Phys. Lett. 63 (1979) 543–548.
[3] S.S. Atik, M. Nam, L.A. Singer, Chem. Phys. Lett. 65 (1979) 75–80.
[4] N.J. Turro, A. Yekta, J. Am. Chem. Soc. 100 (1978) 5951–5952.
[5] D.J. Miller, U.K.A. Klein, Ber. Bunsen-Ges. Phys. Chem. 84 (1980) 1135.
[6] P.K.F. Koglan, D.J. Miller, J. Steinwandel, M. Hauser, J. Phys. Chem. 85 (1981) 2363–2366.
[7] P. Lianos, M. Dinh-Cao, J. Lang, R. Zana, J. Chim. Phys. Phys. Chim. Biol. 78 (1981) 497–501.
[8] F.M. Winnik, Chem. Rev. 93 (1993) 587–614.
[9] G.B. Behera, B.K. Mishra, P.K. Behera, M. Panda, Adv. Colloid Interf. Sci. 82 (1999) 1–42.
[10] A. Nakajima, Bull. Chem. Soc., Jpn. 44 (1971) 3272–3277.
[11] K. Kalyanasundaram, M. Gratzel, J.K. Thomas, J. Am. Chem. Soc. 96 (1974) 7869–7874.
[12] K. Kalyanasundaram, J.K. Thomas, J. Am. Chem. Soc. 99 (1977) 2039–2044.
[13] W. Dannhauser, Z. Phys. Chem., Bd. 213 (1959) 225–230.
[14] M. Omini, Physica A 83 (1976) 431–453.
[15] G. Vicq, A.M. Bottreau, J.M. Fornies-Marquina, J. Mol. Liq. 38 (1988) 233–265.
[16] C. Honda, M. Itagaki, R. Takeda, K. Endo, Langmuir 18 (2002) 1999–2003.
[17] H.J. Pownall, L.C. Smith, J. Am. Chem. Soc. 95 (1973) 3136–3140.
[18] B.K. Selinger, A.R. Watkins, J. Photochem. 16 (1981) 321–330.
[19] D.J. Miller, Ber. Bunsen-Ges. Phys. Chem. 85 (1981) 337–340.
[20] B.K. Selinger, A.R. Watkins, J. Photochem. 20 (1982) 319–325.
[21] L.M. Almeida, W.L.C. Vaz, K.A. Zachariasse, V.M.C. Madeira, Biochemistry 21 (1982) 5972–5977.
[22] P. Lianos, M.-L. Viriot, R. Zana, J. Phys. Chem. 88 (1984) 1098–1101.
[23] R. Zana, J. Phys. Chem. B 103 (1999) 9117–9125.
[24] M. Aoudia, M.A.J. Rodgus, W.H. Wade, J. Phys. Chem. 88 (1984) 5008–5012.
[25] K.A. Zachariasse, Trend Photochem. Photobiol. 3 (1994) 211.
[26] K. Bhattacharyya, B. Bagchi, J. Phys. Chem. A 104 (2000) 10603–10613.
[27] K. Bhattacharyya, Accounts Chem. Res. 36 (2003) 95–101.
[28] N.E. Levinger, Curr. Opin. Colloid Interf. Sci. 5 (2000) 118–124.
[29] M. Rusdi, Y. Moroi, T. Hlaing, K. Matsuoka, Bull. Chem. Soc., Jpn. 78 (2005) 604–610.
[30] Z. Zhang, G. Xu, F. Wang, G. Du, J. Dispers. Sci. Technol. 26 (2005) 297–302.
[31] K. Toerne, R. Rogers, R. von Wandruszka, Langmuir 17 (2001) 6119–6121.
[32] P.H. Elworthy, C.B.J. Macfarlane, J. Chem. Soc. (1963) 907–914.
[33] P. Becher, in: M.J. Schick (Ed.), Nonionic Surfactants, Marcel Dekker, New York, 1963, p. 478.
[34] N.J. Turro, P.-L. Kuo, Langmuir 1 (1985) 170–172.
[35] A. Nakajima, J. Lumin. 11 (1976) 429–432.
[36] A. Nakajima, Kagaku Ryoiki. 33 (1979) 394–401.
[37] R.D. Wanchope, F.W. Getzen, J. Chem. Eng. Data 17 (1972) 38–41.
[38] R. Wans, W.E. Acree Jr., K.W. Street Jr., Analyst 113 (1988) 1465–1467.
[39] K. Hara, W.R. Ware, Chem. Phys. 51 (1980) 61–68.
[40] T.T. Ndou, R. von Wandruszka, J. Lumin. 46 (1990) 33–38.
[41] M. Tachiya, Chem. Phys. Lett. 33 (1975) 289–292.
[42] P.P. Infelta, M. Grazel, J. Chem. Phys. 70 (1979) 179–186.
[43] B. Stevens, M.I. Ban, Trans. Faraday Soc. 60 (1964) 1515–1523.
[44] J.B. Birks, L.G. Christophorou, Proc. R. Soc. London, Ser. A 274 (1963) 552–565.
[45] J.B. Birks, D.J. Dyson, Proc. R. Soc. London, Ser. A 275 (1963) 135–148.
[46] J.B. Birks, L.G. Christophorou, Proc. R. Soc. London, Ser. A 277 (1963) 571–583.
[47] J.B. Birks, M.D. Lumb, I.H. Munro, Proc. R. Soc. London, Ser. A 280 (1964) 289–297.
[48] H.-J. Galla, E. Sackmann, Biochim. Biophys. Acta 339 (1974) 103–115.
[49] J.M.G. Martinho, J.P. Farinha, M.N. Berberan-Santos, J. Duhamel, M.A. Winnik, J. Chem. Phys. 96 (1992) 8143–8149.
[50] A. Malliaris, J. Le Moigne, J. Sturm, R. Zana, J. Phys. Chem. 89 (1985) 2709–2713.
[51] C. Honda, H. Kamizono, K. Matsumoto, K. Endo, J. Colloid Interf. Sci. 278 (2004) 310–317.
[52] P. Sen, S. Mukherjee, A. Haider, K. Bhattachayya, Chem. Phys. Lett. 385 (2004) 357–361.